HHS Public Access

Author manuscript

J Control Release. Author manuscript; available in PMC 2016 February 10.

Published in final edited form as:

J Control Release. 2015 February 10; 199: 145–155. doi:10.1016/j.jconrel.2014.12.013.

Biodistribution and Delivery Efficiency of Unmodified Tumor-Derived Exosomes

Tyson Smyth[1], **Max Kullberg**[1], **Noeen Malik**[2], **Peter Smith-Jones**[3], **Michael W. Graner**[4], and **Thomas J. Anchordoquy**[1]

[1]University of Colorado Denver, Anschutz Medical Campus, Department of Pharmaceutical Sciences, Aurora, CO, USA

[2]Ulm University Hospital, Clinic for Nuclear Medicine, Ulm, Germany

[3]Stony Brook School of Medicine, Department of Psychiatry, Stony Brook, NY, USA

[4]University of Colorado Denver, Anschutz Medical Campus, Department of Neurosurgery, Aurora, CO, USA

Abstract

The use of exosomes as a drug delivery vehicle has gained considerable interest. To establish if exosomes could be utilized effectively for drug delivery, a better understanding of their *in vivo* fate must be established. Through comparisons to liposomal formulations, which have been studied extensively for the last thirty years, we were able to make some comprehensive conclusions about the fate of unmodified tumor-derived exosomes *in vivo*. We observed a comparable rapid clearance and minimal tumor accumulation of intravenously-injected exosomes, PC:Chol liposomes, and liposomes formulated with the lipid extract of exosomes, suggesting the unique protein and lipid composition of exosomes does not appreciably impact exosomes' rate of clearance and biodistribution. This rapid clearance along with minimal tumor accumulation of unmodified exosomes limits their use as an anti-cancer drug delivery vehicle; however, when delivered intratumorally, exosomes remained associated with tumor tissue to a significantly greater extent than PC:Chol liposomes. Furthermore, experiments utilizing mice with impaired adaptive or innate immune systems, revealed the significance of the innate immune system along with the complement protein C5 on exosomes' rate of clearance.

Keywords

Exosomes; Liposomes; Biodistribution; Intravenous Injection; Intratumoral Injection

To whom correspondence should be addressed: Thomas Anchordoquy, 12850 Montview Blvd., University of Colorado Denver, School of Pharmacy, Aurora, CO 80045, Tom.Anchordoquy@ucdenver.edu, Phone: 303-549-8046.

Introduction

The growing evidence of exosomes' innate ability to deliver naturally incorporated cargo to recipient cells has excited the drug delivery field [1–11]. Furthering this interest is the belief that exosomes are stable *in vivo*, as exosomes can be isolated from a multitude of biological fluids, including blood, urine, saliva, milk, and pleural effusions [12–14]. In addition, patient-derived exosomes are postulated to be immune compatible, which would be an advantage over current nanoparticle systems [15]. Given the excitement surrounding exosomes, it is not surprising that several groups have already used the vesicles to deliver therapeutics in animal models [16–20]. However, a better understanding of exosomes' *in vivo* targets and mechanism of clearance is needed to foster the development of exosomes as a drug delivery vehicle.

Exosomes closely resemble liposomes in size and membrane structure. However, while exosomes have only recently been proposed for use in drug delivery, liposomes have been thoroughly investigated as a drug delivery vehicle for over thirty years. Despite the duration of this investigation, relatively few liposomal formulations have made it to the market. The rapid clearance of liposomes by the reticuloendothelial system (RES), overestimation of the enhanced permeation and retention (EPR) effect, and minimal cell penetration after extravasation from blood vessels by both passively and actively targeted liposomes, have prevented liposomes from becoming ubiquitous in cancer therapies [21]. It has been postulated that exosomes may avoid some of the pitfalls of liposomes due to their unique lipid and protein compositions. However, recent biodistribution studies of intravenously injected exosomes [19, 20, 22, 23], along with our own results, demonstrate the rapid clearance of exosomes by the liver and spleen.

We believe the importance of the unique composition of exosomes may be elucidated through comparisons with specific liposomal formulations. Here we demonstrate that the biodistribution and clearance of exosomes injected intravenously resembles that of various liposome formulations. The clearance of exosomes appears to be regulated, at least in part, by the innate immune system, likely mediated by complement opsonization. Furthermore, intravenous injection of exosomes had no greater accumulation in tumor tissue than liposomes; however, when delivered intratumorally, exosomes remain associated with tumors to a significantly greater extent than liposomes. This led us to compare the ability of unmodified tumor-derived exosomes loaded with doxorubicin with liposomal doxorubicin formulations to treat subcutaneous tumors when injected intratumorally.

Materials and Methods

Materials

L-α-phosphatidylcholine (Chicken Egg) (PC), L-α-phosphatidylserine (Porcine Brain) (PS), sphingomyelin (Porcine Brain) (SM), 1,2-dioleoyl-*sn*-glycero-3-phosphoethanolamine (DOPE), and cholesterol were acquired from Avanti Polar Lipids (Alabaster, AL). Mouse mammary carcinoma (4T1) cells, human mammary adenocarcinoma (MCF-7) cells, and human prostate adenocarcinoma PC3 cells were purchased from ATCC (Manassas, VA). BCA Protein Assay Reagent was purchased from Fisher Scientific (Pittsburgh, PA). Roswell

Park Memorial Institute (RPMI) medium 1640, Dulbecco's Modification of Eagle's Medium (DMEM), Phosphate Buffered Saline (PBS), Fetal Bovine Serum (FBS), Trypsin, and Penicillin-Streptomycin were all obtained from Mediatech, Inc. (Manassas, VA). Plasmocin™ was obtained from InvivoGen (San Diego, CA). DIR (DiIC18(7) (1,1'-Dioctadecyl-3,3,3',3'-Tetramethylindotricarbocyanine Iodide) was acquired from Life Technologies (Carlsbad, CA). Sepharose™ CL-4B was acquired from GE Healthcare (Uppsala, Sweeden). D(+)-Sucrose, 99.7%, for biochemistry, was bought from Acros Organics (Fairlawn, New Jersey). Indium-111 was purchased from Nordion (Ottowa, Canada). P6 size exclusion gel was purchased from BioRad (Hercules, CA). Balb/c, athymic nude (NU/J), and NOD.CB17-Prkdcscid/J mice, 4 weeks of age, were acquired from Jackson Laboratories (Bar Harbor, Maine). Doxorubicin was purchased from Tocris Biosciences (Bristol, United Kingdom). Matrigel was purchased from Corning (Corning, NY).

Exosome Isolation

Exosomes were isolated from the supernatant of 4T1, MCF-7, and PC3 cells as previously described [24]. Briefly, all cell lines were passaged three days prior to collecting the cell culture supernatant, allowing the cells to grow to 75% confluency. All cells were cultured in 5-layer BD tissue culturetreated flasks (875 cm^2). Exosomes were harvested from the cell culture supernatant by a series of centrifugation steps: 10 min at 300 × g, 20 min at 20,000 × g, and 2 hours at 120,000 × g. Concentrated exosomes were washed in 10 ml PBS and centrifuged at 200,000×g for 2 hours on a sucrose density cushion. The sucrose cushion consisted of three layers: 12% sucrose, 30% sucrose, and 50% sucrose. Exosomes have a density ranging from 1.1 to 1.2 g/cm^3 [11, 25, 26]. Therefore, the 30% sucrose fraction and the top of the 50% sucrose fraction were collected, washed with 13 ml PBS, and centrifuged at 120,000×g for 2 hours. The pelleted exosomes were re-suspended in 200 μl PBS. Exosome protein content was quantified using the BCA protein assay.

Lipid Extraction

Lipids from 4T1-derived exosomes were extracted using the Bligh and Dyer method [27]. Briefly, approximately 1 milligram of exosomes (weight based on BCA protein content) in 500 μl PBS was added to 1.9 ml of $CHCl_3$:MeOH at a 1:2 mole ratio and vortexed. An aliquot (625 μl) of $CHCl_3$ was then added to the mixture. A magnetic stir bar was placed in the vial and samples were stirred vigorously for 3 hours. Next, 625 μl dH_2O was added and stirred vigorously for one additional hour. The sample was then centrifuged to separate the aqueous and organic phases. The organic phase was recovered and washed with 625 μl dH_2O. The organic phase was then removed and dried under a nitrogen stream.

Liposome Preparation

Three liposomal formulations were used in this work. The first was synthesized from the lipid extracts of 4T1 exosomes. The second was formulated to mimic the lipid composition of exosomes [24, 28–32]. The third was a PC:Chol liposome. PC:Chol liposomes have been extensively studied and can be used for comparison to previous reports. To mimic the lipid composition of exosomes (SynExoLiposomes), liposomes were formulated with PC/PE/PS/SM/Chol at a mole percentage of 21/17.5/14/17.5/30 [24, 28–32]. PC/Chol

liposomes were formulated at a mole percentage of 67/33. Lipid mixtures in chloroform were dried in glass vials under a nitrogen stream and placed under vacuum to remove residual chloroform. To the glass vials containing the dried lipids, PBS was added and subsequently sonicated to remove lipids from the glass vial walls. The lipid/PBS mixtures were removed and extruded through 100 nm-pore sized polycarbonate membranes (Avestin, Ottawa, ON).

Sizing

The size of exosomes and liposomes was determined using a NanoSight NS300. Exosomes were analyzed prior to and after addition of doxorubicin. One microgram of exosomes (based on protein weight) or one microgram of liposomes was added to 1000 μl PBS. For analysis, samples were infused into the NanoSight NS300 using a syringe pump at a rate of 10 (arbitrary units). Data for each sample was collected for 60 seconds and analyzed using NanoSight NTA 2.3 software.

Fluorescent Labeling of Exosomes and Liposomes

DIR was used to fluorescently label the lipid bilayer of exosomes and liposomes. DIR was incorporated into exosomes at a concentration of 0.5% by weight. Five microliters of DIR, at a concentration of 220 μg/ml in ethanol, were mixed with 220 μg exosomes or liposomes in 100 μl PBS for one hour. Ethanol and any unincorporated DIR was removed using a Sepharose™ CL-4B column conditioned with PBS, pH 7.4. Note: No detectable amount of DIR remained unincorporated with liposomes or exosomes using this method.

Tumor-Bearing Mouse Models

In order to visualize the biodistribution of cancer cell-derived exosomes in tumor-bearing mice, Balb/c, nude, and NOD.CB17-Prkdcscid/J mice were inoculated with either 4T1 cells or PC3 cells. 4T1 cells (5×10^4), maintained in RPMI and supplemented with 10% FBS, were injected into the mammary fat pads of Balb/c, nude, and NOD.CB17-Prkdcscid/J mice in a volume of 30 μl of PBS. PC3 cells were maintained in DMEM and supplemented with 10% FBS. In order to promote tumor formation, PC3 cells were suspended in ice-cold matrigel. PC3 cells (2×10^6) in 200 μl matrigel/PBS, 50/50 (v/v) ratio, were injected subcutaneously into the flanks of nude mice. All procedures were approved by the IACUC committee of The University of Colorado Anschutz Medical Campus, and conformed to the guidelines established by NIH.

In Vivo Imaging

Mice bearing 4T1 tumors in their mammary fat pads were monitored daily. Prior to exosome injection, the ventral hair of Balb/c and NOD.CB17-Prkdcscid/J mice was removed using Nair (Church & Dwight Co., Inc). When tumors reached a volume of 400 mm^3, calculated by $(width)^2 \times length/2$, mice were injected intravenously (tail vein) with 60 μg DIR-labeled exosomes or liposomes in 200 μl PBS. Similarly, 60 μg of DIR-labeled exosomes or liposomes in a volume of 50 μl PBS were injected intratumorally in Balb/c mice bearing ≈ 400 mm^3 4T1 tumors. The biodistribution of exosomes or liposomes, in live mice under isoflurane anesthesia, injected either intravenously or intratumorally was determined using

an IVIS 200 Optical Imaging System (Xenogen, Caliper Life Sciences). Fluorescent background subtraction was performed, and the data displayed on a linear scale. At the conclusion of each study, organs were excised and their fluorescence imaged. Live Image 4.2 Software was used for quantitative analysis. All mice were imaged with identical instrument settings. Allowing for direct comparison, using scale bars, of the mice within a sample group at each defined time point.

Radiolabeling of Exosomes and Liposomes

Indium-oxine was prepared as previously reported [33]. Briefly, ^{111}In (4 mCi, 13 μL, 10 mM HCl) was mixed with 10 μL of an 8 mM ethanolic solution of 8-hydroxyquinoline and 150 μL of 0.2 M sodium acetate. This solution was extracted with 0.5 mL of chloroform and the organic layer dried under vacuum at 40 °C for 20 minutes. The residue was dissolved by adding 200 μL of 25 mM HEPES and briefly vortexing. The [^{111}In]oxine was used immediately. Radiolabeling of the exosomes or liposomes (2.5–3.7 mg/mL) was performed by adding the reconstituted [^{111}In]oxine at a ratio of 320 μCi ^{111}In/mg exosome (or liposome). After briefly vortexing, the solutions were allowed to stand at ambient temperature for 20 minutes before being purified on a 10 mL P6 column eluted with phosphate buffered saline. One ml fractions were collected and the two main ^{111}In-labeled exosome (or liposome) fractions pooled. The labeling efficiencies were 81%, 67%, and 61% for the PC3-exosomes, MCF7 exosomes and liposomes, and specific activity was 270, 220, and 180 μCi/mg, respectively.

In Vivo Biodistribution of Radio-Labeled Exosomes and Liposomes

Nude mice were injected with 130–140 μL of [^{111}In]PC3-exosomes (7.6 μCi, 30 μg), [^{111}In]MCF7-exosomes (7.2 μCi, 32 μg), or [^{111}In]liposomes (6.1 μCi, 34 μg) in the tail vein. The syringes were measured in a CRC 25 dose calibrator (Capintec, Ramsey, NY) before and after injection. A standard of 0.76 μCi [^{111}In]Cl_3 was prepared at the time of injection and diluted to 1 ml. Serial blood samples (25–30 μL) were collected from the mice at 0.5, 1.5, 3, and 7 hours post injection by the modified tail clip method [34]. After 24 hours, the whole body retention of ^{111}In in the mice was measured in a dose calibrator and the mice were sacrificed by CO_2 asphyxiation followed by cervical dislocation. Blood samples were immediately drawn by cardiac puncture and the mice were subjected to a full necropsy. Samples of all organs were collected, weighed, and counted in a 2480 Wizard gamma counter (Perkin Elmer, Waltham, MA) along with the blood samples and ^{111}In standard. The gamma counter data was converted to a percentage of the injected dose (%ID) by considering the known activity injected and reference standard activity and the cpm of the organ and reference standard. The blood clearance data is expressed as %ID in blood. The total weight of blood in mice is estimated to be 5.5 ml/100 g [35]. Biodistribution data is expressed as a %ID/g of organ tissue.

Doxorubicin Loading into Exosomes

To 200 μl PBS containing 450 μg exosomes, 20 μl doxorubicin HCl, at 250 μg/ml in PBS, was added at 37°C. Samples were vortexed and incubated at 37°C for 2 hours. After incubation, samples were run through a Sepharose™ CL-4B column conditioned with PBS to remove unincorporated free doxorubicin. To measure the extent of doxorubicin

association with exosomes, a UV spectrophotometer (Agilent 8453 UV-visible Spectroscopy System) was used. Absorbance, not fluorescence, was used to measure doxorubicin association with exosomes because we were concerned that the fluorescence of doxorubicin might be quenched, at least partially, after association with exosomes. The molar extinction coefficient of doxorubicin (10,000 cm-1M-1 at 480 nm) was used to calculate the molar concentration of doxorubicin associated with exosomes. Using this method, doxorubicin was associated with exosomes at roughly 5% by weight.

Doxorubicin Loading into Liposomes

Liposomes were actively loaded with doxorubicin as previously described [36, 37]. Briefly, SynExoLiposomes and PC:Chol (mole ratio 2:1) liposomes were hydrated with 300 mM ammonium sulfate. Liposomes were subsequently prepared as described above. To remove ammonium sulfate from the extra-liposomal solution, liposomes were run through a Sepharose™ CL-4B column conditioned with PBS, pH 7.4. Subsequently, to 200 μl of PBS containing 450 μg of liposomes, 9 μl doxorubicin HCl at 2.5 mg/ml was added. Samples were then incubated at 60°C for 20 minutes. To remove unincorporated free doxorubicin, samples were run through a Sepharose™ CL-4B column conditioned with PBS, pH 7.4. Fluorescence was used to measure the incorporation of doxorubicin into liposomes. Using a Fluoromax, (Photon Technology International, Birmingham, New Jersey) with 2 nm slit widths, samples were excited at 480 nm and emission monitored at 565 nm. To ensure doxorubicin was not being quenched, liposomes were mixed with Triton X at a final concentration of 0.5% and vortexed for one minute prior to analysis. A standard curve of free doxorubicin was used to calculate the molar concentration of doxorubicin in each liposome sample.

Doxorubicin Release

To simulate *in vivo* conditions, exosomes and liposomes loaded with doxorubicin were stored in FBS/PBS (50/50 v/v ratio) and divided into 15 identical aliquots at 37°C. At times 0, 1, 3, 7, and 24 hours, exosome or liposome samples, in triplicate, were passed through a Sepharose™ CL-4B column conditioned with PBS to remove released doxorubicin. The extent of doxorubicin incorporated in exosomes and liposomes at each time point was measured as described above.

Therapeutic Experiments

Balb/c mice bearing 4T1 tumors were randomly split into six groups and received one of the following treatments in a volume of 50 μl PBS; 1 mg/kg free doxorubicin, 5 mg/kg free doxorubicin, 1 mg/kg doxorubicin loaded into 400 μg PC:Chol liposomes, 1 mg/kg doxorubicin loaded into 400 μg synthetic exosomes liposomes (SynExoLipsomes), 1 mg/kg doxorubicin loaded into 400 μg 4T1 exosomes, or control (PBS). All treatments were administered intratumorally on days 7, 11, and 15. Day zero was the day of tumor inoculation.

Results

Generation of Exosomes and Liposomes

Exosomes were purified from the cell culture supernatant of 4T1, PC3, and MCF-7 cells by a series of ultracentrifugation steps as described above. Our previous work has thoroughly demonstrated the presence of exosomes in our samples through the use of electron microscopy, western blot analysis, nanoparticle tracking analysis, and mass spectrometry [24, 38]. Liposomes in this work were prepared to either mimic the lipid composition of exosomes (SynExoLiposomes) [24, 28–32], or to be comparable to a widely studied liposomal formulation, PC:Chol. Additionally, liposomes were created from the lipid extracts of exosomes. Tumor-derived exosomes have a distinct protein and lipid composition resembling that of the cells from which they are derived. It has been postulated that the unique lipid composition may play a role in exosome uptake and fusion with recipient cells [39]. While there does not appear to be a highly conserved lipid composition of exosomes derived from various cell types, some general trends are apparent. Exosomes have relatively high cholesterol content when compared to the lipid content of cell plasma membranes, constituting approximately 30% of exosomal lipids. Additionally, there is a two fold increase in the content of anionic lipids, most notably phosphatidylserine (PS). Similarly, sphingomyelin (SM) increases 2.5 fold in exosomes compared to the plasma membrane. The increase of cholesterol, PS, and SM all come at the cost of phosphatidylcholine (PC). Liposomes were formulated to mimic the lipid composition of exosomes (SynExoLiposomes). Furthermore, PC:Chol liposomes, were prepared allowing us to compare our observations to previous reports. Lastly, liposomes were formulated from the lipid extracts of 4T1 exosomes. While we did not analyze the lipid content of extracted lipids, we expect the lipid composition to be similar to what has been reported in the literature, and to have a matching lipid composition to 4T1 exosomes. Liposomes made from exosome lipid extracts will be referred to as ‘exoliposomes’. The sizes of all exosomes and liposomes used in this work, as measured by Nanosight, are presented in Figure 1. The negligible size differences between exosomes and liposomes allowed us to attribute any changes in biodistribution profiles and clearance rates to the physical properties of exosome and liposomal formulations.

Biodistribution of Exosomes and Liposomes

In order to compare the biodistribution of systemically delivered exosomes, to exoliposomes, and to PC:Chol liposomes, a tumor bearing mouse model was established. Balb/c mice, 4 weeks of age, were inoculated with 4T1 cells in the mammary fat pad. When tumors reached a volume of 400 mm^3, 15 days after inoculation, mice were intravenously injected with 4T1 exosomes, 4T1 exoliposomes, or PC:Chol liposomes. Exosomes and liposomes were labeled with the lipophilic fluorescent tracer DIR. Long-chain dialkylcarbocyanines, such as DIR, are used extensively to label biological membranes, including exosomes and liposomes, for *in vitro* and *in vivo* tracking [20, 32, 40–44]. Balb/c mice intravenously injected with exosomes and liposomes were imaged using an IVIS 200 Optical Imaging System at 1, 8, and 24 hours post injection. At the 24 hour time point, the mice were sacrificed and organs excised. One hour after intravenous injection, the majority of exosomes appeared to have accumulated in the liver and spleen. In fact, over the course

of 24 hours, we saw a decrease in fluorescence suggesting peak accumulation in liver and spleen occurred prior to the one hour time point. It is possible that the decrease in fluorescence over the course of the experiment was due to degradation of the fluorescent tracer DIR. Regardless, our results demonstrate the rapid uptake of exosomes by the liver and spleen, consistent with previous reports examining the biodistribution of exosomes [20, 22, 23]. Interestingly, we observed a similar biodistribution profile for exoliposomes and PC:Chol liposomes. Both liposome formulations were rapidly taken up by the liver and spleen with no observable accumulation in tumor tissue. A necroscopy of the mice from each sample set revealed the significant uptake of exosomes and liposomes by the liver and spleen along with limited uptake by the lungs and kidneys. However, no accumulation was observed in tumor tissue (Figure 2).

To further characterize the biodistribution of exosomes and liposomes *in vivo*, PC3 exosomes, MCF-7 exosomes, and PC:Chol liposomes were radiolabel with indium-111 and injected intravenously into nude mice bearing PC3 tumors or non-tumor bearing nude mice. In order to incorporate indium-111 into exosomes and liposomes, indium-111 was complexed to oxine molecules. Complexation with oxine, a hydrophobic molecule, allowed indium-111 to partition into the lipid bilayer of exosomes and liposomes. Indium-111 oxine complexes have previously been used to study the biodistribution of liposomes and cells *in vivo* [45–47]. Exosomes derived from both PC3 and MCF-7 cells were included in this experiment to elucidate any difference in the biodistribution of exosomes derived from the same cell lines as the tumor to that of any other origin. Furthermore, we aimed to identify any difference in exosome blood clearance and biodistribution profiles of tumor and non-tumor bearing nude mice. The presence of a tumor may saturate the immune systems with tumor-derived exosomes, thereby reducing the rate of clearance of intravenously injected tumor-derived exosomes.

Four week old nude mice, either non-tumor bearing or bearing a PC3 tumor, with an average volume of 250 mm^3, were intravenously injected with radiolabeled PC3 exosomes, MCF-7 exosomes, or PC:Chol liposomes (Figure 3). Blood clearance of exosomes and liposomes was monitored over the course of 24 hours. At 24 hours post injection, the mice were sacrificed and organs excised and analyzed. Data analysis revealed the rapid blood clearance of both PC3 exosomes and MCF-7 exosomes along with PC:Chol liposomes in PC3 tumor bearing nude mice (Figure 3A). Less than 5% of the injected dose remained three hours post injection for both exosome types and PC:Chol liposomes. The rapid removal of PC:Chol liposomes from circulation and the limited accumulation of PC:Chol liposomes in tumor tissue, less than 2% of the injected dose per gram of tumor tissue, is similar to what has been observed previously for PC:Chol liposome formulations [48–50]. Furthermore, the biodistribution profile of PC3 exosomes, MCF-7 exosomes, and PC:Chol liposomes 24 hours after intravenous injection (Figure 3B) appeared similar to the biodistribution profile we observed with 4T1 exosomes injected into Balb/c mice (Figure 2), where a higher proportion of exosomes appear to be associated with the liver, spleen and even the kidneys than other organs, including PC3 tumors (Figure 3B). Additionally, the presence of a tumor did not significantly affect the blood clearance of exosomes (Figure 3C) and we saw little

difference in the biodistribution profile of PC3 exosomes in mice bearing PC3 tumors and non-tumor bearing mice (Figure 3D).

Influence of the Immune System on Exosomes Clearance

In order to investigate the impact of the innate immune systems on exosome clearance and biodistribution in tumor-bearing mice, we intravenously injected 4T1 exosomes into Balb/c, nude and NOD.CB17-Prkdcscid/J mice. Each mouse strain was inoculated with a 4T1 tumor in the mammary fat pad. Comparison of nude mice, which suffer from a lack of adaptive immunity, along with NOD.CB17-Prkdcscid/J, which suffer from impaired innate immunity including impaired complement activity [51], with healthy Balb/c mice revealed the significance of the innate immune systems and complement on the rapid uptake of exosomes by the RES. Complement has been widely shown to mediate clearance of liposomal systems [52–57], suggesting activation of the complement system may also play an integral role in exosome clearance and biodistribution. In fact, exosomes have previously been shown to bind complement proteins *in vitro* and *in vivo* [58, 59]. 4T1 exosomes in Balb/c mice were taken up by the liver and spleen as fast as 20 minutes post injection, with little to no change over the course of 2 hours. A similar biodistribution pattern was observed in nude mice, suggesting the adaptive immune system is not responsible for the clearance of exosomes. Yet, in NOD.CB17-Prkdcscid/J mice, an increase in accumulation of 4T1 exosomes in the liver and spleen occurred between 20 minutes and 2 hours post injection (Figure 4). The slower uptake of exosomes by the RES in mice with an impaired innate immune system and a complement deficiency, suggests that the innate immune system, with help from complement opsonization, contributes to the removal of tumor derived exosomes from circulation.

Use of Exosomes as a Drug Delivery Vehicle

Our initial interest in exosomes was to explore their use as a drug delivery vehicle. However, based on our biodistribution studies, unmodified exosomes appear to be incapable of tumor-specific delivery. In addition to poor tumor targeting, over-dosing of exosomes has severe negative consequences. In our preliminary investigations, we observed what appeared to be asphyxiation of mice when 400 μg of syngeneic exosomes were injected intravenously. A shortness of breath along with heavy breathing was observed for approximately five minutes before mice recovered. While an injection dose of 60 μg had no observable side effects. In order to identify the cause of what appears to be asphyxiation, we injected one mouse with 400 μg DIR-labeled exosomes (Figure 5). Sadly, the mouse died within three minutes post injection. Imaging of the excised organs of the mouse revealed the accumulation of exosomes in the lungs.

Intratumoral Injection of Exosomes and Liposomes

Our previous work has demonstrated the superior association and internalization of exosomes compared to PC:Chol liposomes *in vitro* [24], suggesting exosomes injected intratumorally may associate with tumor cells to a greater extent than PC:Chol liposomes of a similar size. Balb/c mice bearing 400 mm^3 4T1 tumors were injected intratumorally with 4T1 exosomes and PC:Chol liposomes labeled with equal concentrations of DIR. Mice were

imaged at 1, 12, and 24 hours post injection (Figure 6A) before organs were excised and imaged (Figure 6B). Analysis of the excised tumors indicates that exosomes stay associated with the tumors to a significantly greater degree than PC:Chol liposomes (Figure 6C). Our results suggest that the protein and lipid composition of exosomes allow for efficient uptake by tumor cells when compared to liposomes.

Anti-Tumor Efficacy of Doxorubicin-Loaded Exosomes

We next aimed to investigate whether exosomes could deliver doxorubicin more efficiently and have a greater impact on tumor size than liposomes when injected intratumorally. In order to load exosomes with doxorubicin, we initially tried electroporation. Electroporation has been previously employed to load siRNA into exosomes [18], and more recently to load doxorubicin [20]. Unfortunately, in our hands, electroporation was unsuccessful. However, we found that at high doxorubicin concentrations (250 μg/ml), doxorubicin spontaneously incorporated into exosomes. Doxorubicin consistently incorporated into exosomes at 5 ± 1 μg per 100 μg of exosomes. PC:Chol liposomes along with SynExoLiposomes were loaded with doxorubicin at a matching doxorubicin concentration of 5 μg doxorubicin per 100 μg liposomes, using well characterized pH loading techniques [36, 37]. Doxorubicin loaded exosomes and liposomes were incubated in 50% fetal bovine serum to simulate the presence of proteins in the intratumoral microenvironment. The release profiles of doxorubicin from 4T1 exosomes and PC:Chol liposomes in 50% (v/v) FBS/PBS paralleled one another over the course of 24 hours (Figure 7A). After 3 hours incubation at 37°C, approximately 45% of doxorubicin had been released from both 4T1 exosomes and PC:Chol liposomes, while only 25% of doxorubicin had leaked from SynExoLiposomes at 3 hours. Further, after 24 hours incubation, 30% of doxorubicin remained in 4T1 exosomes while approximately 20% remained in PC:Chol liposomes. Again, more doxorubicin remained entrapped in SynExoLiposomes (40%) after 24 hours incubation than both 4T1 exosomes and PC:Chol liposomes. The release profile of doxorubicin from PC:Chol liposomes in the presence of 50% serum is consistent with what has been reported in the literature [60, 61]. The slower leakage of doxorubicin from SynExoLiposomes compared to PC:Chol liposomes suggests the unique lipid composition confers stability and decreased permeability of incorporated material under *in vivo* conditions.

To test the anti-tumor efficacy of exosomes loaded with doxorubicin in comparison to doxorubicin loaded liposomes of a similar size, Balb/c mice, inoculated with 4T1 tumor cells in the mammary fat pad were randomly split into six treatment groups. When tumors became palpable, seven days after inoculation, treatment was initiated. Mice received intratumoral injections on days 7, 11, and 15 with either (I) control PBS; (II) free doxorubicin 1 mg/kg; (III) free doxorubicin 5 mg/kg; (IV) 4T1 exosomes loaded with 1 mg/kg doxorubicin; (V) PC:Chol liposomes loaded with 1 mg/kg doxorubicin; and (VI) SynExoLiposomes loaded with 1 mg/kg doxorubicin. Tumors volumes were measured every three days. There was a clear suppression of tumor growth in all mice receiving doxorubicin compared to controls. Further, tumor suppression of mice receiving 5 mg/kg free doxorubicin was significantly better than all other treatment groups. However, there was no significant decrease in tumor growth in mice that received exosomes or liposomes loaded with doxorubicin when compared to free drug at the same concentration. Interestingly,

exosomes loaded with doxorubicin suppressed tumor growth significantly better than PC:Chol liposomes (Figure 7B), as was hypothesized based on the greater retention of exosomes in the tumor tissue compared to PC:Chol liposomes (Figure 6).

Discussion

Exosomes are complex vehicles with an abundance of incorporated proteins and a unique lipid composition. The intricate combination of lipids and proteins makes elucidating their biological functions difficult. A huge effort has taken place over the last decade to characterize exosomes from various origins in order to gain insight into exosomes' biological significance. Our research, aimed at exploiting exosomes' drug delivery potential, has taken a more global approach in studying the importance of proteins and lipids in tumor-derived exosomes. In order for unmodified exosomes to be used as a drug delivery vehicle, we needed to first study their biodistribution profiles when injected intravenously. Through comparison of biodistribution profiles of tumor-derived exosome to that of specific liposomal formulations, we were able to make some general conclusions about the importance of the protein and lipid components of exosomes.

The elevated levels of signal transduction, migration, adhesion, and antigen presentation proteins incorporated into the lipid membrane of exosomes, compared with proteins of various other biological functions [62–64], suggests exosomes may be important for cellular communication both locally between neighboring cells and to distant cellular targets. Here, we have shown that tumor-derived exosomes, in multiple mouse models, have similar biodistribution profiles to liposomes made from the lipid extract of exosomes (exolipsomes) and to PC:Chol liposomes. The similar rapid uptake of exosomes to exoliposomes, suggests that the protein composition of exosomes does not significantly impact the rate of exosome clearance by the RES. The rapid uptake of exosomes by the RES suggests that exosomes' primary function is not likely communication with distant cellular targets, but possibly to exchange information with neighboring cells and cells of the immune system. Exosomes have been implicated in many immune-regulatory processes, including exposing activating ligands to NK cells and macrophages, transferring antigens to dendritic cells to allow activation of specific T cells, and direct T-cell activation [64–66].

Along with protein profile, it has been suggested that the unique lipid composition of exosomes may influence their *in vivo* circulation times. While there does not appear to be a conserved lipid composition for exosomes derived from different cells types, there does appear to be some general trends, including elevated cholesterol, sphingomyelin (SM), and anionic lipids in comparison to that of the plasma membrane of the cells from which the exosomes were derived [24, 28–32]. Drawing from liposomal literature, it is well known that incorporation of cholesterol and SM into liposomes decreases the rate of clearance of liposomes by the RES [67–69], while the incorporation of the anionic phospholipid phosphatidylserine (PS) increases the rate of clearance [70]. In fact, PS receptors on macrophages have been shown to bind PS in exosomes *in vitro*, likely having a negative impact on exosome circulation times *in vivo* [71]. To investigate the importance of the lipid composition of exosomes with respect to *in vivo* circulation, PC:Chol liposomes and liposomes formulated from the lipid extracts of 4T1 exosomes (exoliposomes) were

intravenously injected into Balb/c mice. The comparable biodistribution profile of exoliposomes to PC:Chol liposomes (Figure 2) implies that the unique lipid composition of exosomes does not considerably impact exosome circulation times in blood.

We next set out to test if tumors can saturate the host immune system with exosomes by constantly releasing tumor-derived exosomes into the circulation, potentially leading to a decrease in the clearance rate of intravenously injected exosomes derived from the same cells as the tumor. To test our hypothesis, radiolabeled PC3-derived exosomes were injected into nude mice bearing a PC3 tumor or into non-tumor bearing nude mice. Nude “NU/J” mice are athymic but have B, NK, and antigen presenting cells, as well as complement activity. The blood clearance profiles of tumor-derived exosomes in tumor and non-tumor bearing mice were identical. This suggests that the continual release of exosomes from tumors into circulation does not saturate the RES, nor has the immune system become accustomed to the presence of tumor-derived exosomes. Additionally, there was no change in the biodistribution of exosomes in tumor-bearing mice and non-tumor bearing mice.

In a similar experiment, we investigated whether exosomes from the same cell line as a tumor in a mouse model, or of other origin, accumulated in the tumor tissue to a greater extent. We found no difference in the accumulation of PC3 exosomes in PC3 tumors in comparison to MCF-7 exosomes, nor was there any difference in the rate of exosome clearance. However, there was some difference in the biodistribution profile between exosome types. PC3 exosomes, from the same cell line as the xenograft tumor, were taken up to a greater extent in the liver and to a lesser extent in the spleen, compared to MCF-7 exosomes. These results suggest that there may be some differences in how each of the two exosome types interacts with the RES. It is also important to point out that these experiments utilized human tumors and exosomes derived from human tumors in a mouse model. While the species differences between the exosomes and animal model (i.e., human vs. mouse) could contribute to the results described here, experiments with exosomes derived from mouse tumors (4T1) exhibited a similar biodistribution profile (described below).

In addition to having similar clearance and biodistribution profiles, both exosomes and PC:Chol liposomes only minimally accumulated in tumor tissue after 24 hours circulation (Figure 3B). The limited accumulation of PC:Chol liposomes per gram of tumor tissue that we observed is consistent with what has previously been observed for similar liposomal formulations [48–50]. Likewise, a relatively small fraction of the injected dose of PC3 and MCF-7 exosomes accumulated in tumor tissue (Figure 3B). Less than two percent of the injected dose per gram of tumor tissue for both exosomes types, and PC:Chol liposomes was associated with tumor tissue 24 hours post injection. Our results suggest that the use of unmodified exosomes as a tumor drug delivery vehicle is limited due to poor tumor accumulation.

Furthermore, our work suggests that the rate of exosome clearance from circulation is likely controlled, at least in part, by the cells of the innate immune system, facilitated by the opsonization of exosomes with complement proteins, and not through antibody-mediated clearance. The rate of exosome uptake by cells of the RES in the liver and spleen of

NOD.CB17-Prkdcscid/J mice is retarded when compared to Balb/c and nude mice (Figure 4). If exosomes were being cleared by an antibody-mediated response, we would expect the rapid clearance of exosomes in Balb/c mice bearing 4T1 tumors, while a slower rate of exosome clearance would be observed in nude mice bearing 4T1 tumors. The presence of a 4T1 tumor in Balb/c mice would expose the mouse immune system to 4T1 exosomes, potentially resulting in an antibody response. We observed no apparent difference in the uptake of exosomes by the RES in Balb/c and nude mice, suggesting antibodies were not responsible for exosome clearance. Furthermore, NOD.CB17-Prkdcscid/J mice suffer from impaired natural killer cell function, a functionally less mature macrophage population, and are deficient for the complement protein C5 [51]. C5 is required for hemolytic complement activity [51], acts as a chemoattractant for cells of the RES [72], and promotes phagocytosis [73–75]. Work with liposomal formulations has demonstrated that the deposition of complement proteins to the surface of liposomes plays an integral role in their clearance by the RES [52–57]. Because exosomes resemble liposomes, it is likely that exosomes also activate the complement system. In fact, complement proteins have been shown to be associated with exosomes *in vitro* and *in vivo* [58, 59]. The impaired rate of exosome uptake in NOD.CB17-Prkdcscid/J mice suggests that the innate immune system, along with complement protein C5, is involved in the clearance of exosomes by the liver and spleen. For a comprehensive view of exosome interactions with the immune system, please see the works of Thery et al., [64] and Robbins et al. [66].

In a preliminary investigation, we attempted to intravenously inject a bolus dose upwards of 400 μg exosomes into the tail vein of Balb/c mice. Surprisingly, we found that injection of over 400 μg of syngeneic exosomes caused the rapid asphyxiation of mice. Numerous studies have injected exosomes intravenously; however, we have not come across a report that has described these types of negative consequences. This is likely due to the fact that most studies intravenously inject less than 100 μg/mouse [18, 19, 22, 76–78] with one study using as much as 200 μg/mouse [79]. We postulate two possible explanations for the observed results: exosomes may be aggregating in lung tissue upon first passage through the lungs, or exosomes are aggregating after intravenous injection and accumulating in the lungs. Both scenarios would result in the asphyxiation of the mice. This post injection aggregation phenomena has been observed with liposomal and lipoplex systems [80–83]. We caution future researchers as to the deleterious effects of the intravenous injection of high concentrations of exosomes. In order for exosomes to be used as a therapeutic or drug delivery vehicle, limited bolus dosing or slow infusion may be required, unless very high drug loading can be achieved. However, even with very high drug loading, the rapid clearance by the liver and spleen will likely present toxicity issues for chemotherapeutics.

Our previous work has shown that exosomes associate and internalize with cancer cells to a greater extent than PC:Chol liposomes *in vitro* [24]. Unfortunately, the vast majority of unmodified exosomes injected intravenously are cleared by the RES before reaching tumor tissue, preventing the direct comparison of exosome and liposome uptake by tumors. Exosomes injected intratumorally associated with tumors to a greater extent than PC:Chol liposomes over the course of 24 hours (Figure 6). These observations suggest that exosomes may be more effective at delivering therapeutic material to tumors than liposomes.

However, treatment of a mouse model bearing a 4T1 mammary tumor with 4T1 exosomes, PC:Chol liposomes, or SynExoLiposomes loaded with doxorubicin had no greater impact on tumor growth than free drug; however, exosomes loaded with doxorubicin impaired tumor growth to a significantly greater extent than PC:Chol liposomes (Figure 7B). The decreased tumor growth again suggests that exosomes are associating with tumor tissue to a greater extent than PC:Chol liposomes.

Conclusions

Unmodified tumor-derived exosomes are rapidly taken up by the RES in the liver and spleen when injected intravenously. The rate at which exosomes are cleared from circulation and their biodistribution profile is similar to both PC:Chol liposomes and liposomes made from the lipid extract of exosomes, suggesting that the unique protein and lipid components of tumor-derived exosomes does not promote extended circulation times. Our results suggest that unmodified tumor-derived exosomes cleared, at least in part, by the innate immune system, likely mediated by the complement system. The rapid clearance of unmodified exosomes inhibits their accumulation in tumor tissue to any significant level, limiting their use as a drug delivery vehicle when injected intravenously; however, when injected intratumorally, exosomes remain associated with tumor tissue to a greater extent than PC:Chol liposomes. In fact, unmodified tumor-derived exosomes loaded with doxorubicin were able to inhibit tumor proliferation to a significantly greater extent than doxorubicin loaded PC:Chol liposomes. Finally, we conclude that unmodified exosomes are unlikely to be useful as a systemically administered tumor-specific delivery system.

Acknowledgements

We would like to thank John Carpenter for use of the NanoSight LM20 instrument. We would also like to thank Joe Gomez at the University of Colorado School of Pharmacy Mass Spectrometry Core. This work was supported by grants 1RO1GM093287-01A1 and 1R01EB016378-01A1 from NIH, and an NIH training grant (5 T32 GM 8732).

References Cited

1. Aliotta JM, Pereira M, Johnson KW, de Paz N, Dooner MS, Puente N, Ayala C, Brilliant K, Berz D, Lee D, Ramratnam B, McMillan PN, Hixson DC, Josic D, Quesenberry PJ. Microvesicle entry into marrow cells mediates tissue-specific changes in mRNA by direct delivery of mRNA and induction of transcription. Experimental hematology. 2010; 38:233–245. [PubMed: 20079801]
2. Hergenreider E, Heydt S, Treguer K, Boettger T, Horrevoets AJ, Zeiher AM, Scheffer MP, Frangakis AS, Yin X, Mayr M, Braun T, Urbich C, Boon RA, Dimmeler S. Atheroprotective communication between endothelial cells and smooth muscle cells through miRNAs. Nature cell biology. 2012; 14:249–256.
3. Umezu T, Ohyashiki K, Kuroda M, Ohyashiki JH. Leukemia cell to endothelial cell communication via exosomal miRNAs. Oncogene. 2013; 32:2747–2755. [PubMed: 22797057]
4. Pegtel DM, Cosmopoulos K, Thorley-Lawson DA, van Eijndhoven MA, Hopmans ES, Lindenberg JL, de Gruijl TD, Wurdinger T, Middeldorp JM. Functional delivery of viral miRNAs via exosomes. Proceedings of the National Academy of Sciences of the United States of America. 2010; 107:6328–6333. [PubMed: 20304794]
5. Al-Nedawi K, Meehan B, Micallef J, Lhotak V, May L, Guha A, Rak J. Intercellular transfer of the oncogenic receptor EGFRvIII by microvesicles derived from tumour cells. Nature cell biology. 2008; 10:619–624.

6. Sheldon H, Heikamp E, Turley H, Dragovic R, Thomas P, Oon CE, Leek R, Edelmann M, Kessler B, Sainson RC, Sargent I, Li JL, Harris AL. New mechanism for Notch signaling to endothelium at a distance by Delta-like 4 incorporation into exosomes. Blood. 2010; 116:2385–2394. [PubMed: 20558614]
7. Street JM, Birkhoff W, Menzies RI, Webb DJ, Bailey MA, Dear JW. Exosomal transmission of functional aquaporin 2 in kidney cortical collecting duct cells. The Journal of physiology. 2011; 589:6119–6127. [PubMed: 22025668]
8. Atay S, Gercel-Taylor C, Suttles J, Mor G, Taylor DD. Trophoblast-derived exosomes mediate monocyte recruitment and differentiation. American journal of reproductive immunology. 2011; 65:65–77. [PubMed: 20560914]
9. Webber J, Steadman R, Mason MD, Tabi Z, Clayton A. Cancer exosomes trigger fibroblast to myofibroblast differentiation. Cancer research. 2010; 70:9621–9630. [PubMed: 21098712]
10. Gu J, Qian H, Shen L, Zhang X, Zhu W, Huang L, Yan Y, Mao F, Zhao C, Shi Y, Xu W. Gastric cancer exosomes trigger differentiation of umbilical cord derived mesenchymal stem cells to carcinoma-associated fibroblasts through TGF-beta/Smad pathway. PloS one. 2012; 7:e52465. [PubMed: 23285052]
11. Valadi H, Ekstrom K, Bossios A, Sjostrand M, Lee JJ, Lotvall JO. Exosome-mediated transfer of mRNAs and microRNAs is a novel mechanism of genetic exchange between cells. Nature cell biology. 2007; 9:654–659.
12. Pisitkun T, Shen RF, Knepper MA. Identification and proteomic profiling of exosomes in human urine. Proceedings of the National Academy of Sciences of the United States of America. 2004; 101:13368–13373. [PubMed: 15326289]
13. Lasser C, Alikhani VS, Ekstrom K, Eldh M, Paredes PT, Bossios A, Sjostrand M, Gabrielsson S, Lotvall J, Valadi H. Human saliva, plasma and breast milk exosomes contain RNA: uptake by macrophages. Journal of translational medicine. 2011; 9:9. [PubMed: 21235781]
14. Bard MP, Hegmans JP, Hemmes A, Luider TM, Willemsen R, Severijnen LA, van Meerbeeck JP, Burgers SA, Hoogsteden HC, Lambrecht BN. Proteomic analysis of exosomes isolated from human malignant pleural effusions. American journal of respiratory cell and molecular biology. 2004; 31:114–121. [PubMed: 14975938]
15. van Dommelen SM, Vader P, Lakhal S, Kooijmans SA, van Solinge WW, Wood MJ, Schiffelers RM. Microvesicles and exosomes: opportunities for cell-derived membrane vesicles in drug delivery. Journal of controlled release : official journal of the Controlled Release Society. 2012; 161:635–644. [PubMed: 22138068]
16. Sun D, Zhuang X, Xiang X, Liu Y, Zhang S, Liu C, Barnes S, Grizzle W, Miller D, Zhang HG. A novel nanoparticle drug delivery system: the anti-inflammatory activity of curcumin is enhanced when encapsulated in exosomes. Molecular therapy : the journal of the American Society of Gene Therapy. 2010; 18:1606–1614. [PubMed: 20571541]
17. Zhuang X, Xiang X, Grizzle W, Sun D, Zhang S, Axtell RC, Ju S, Mu J, Zhang L, Steinman L, Miller D, Zhang H-G. Treatment of Brain Inflammatory Diseases by Delivering Exosome Encapsulated Anti-inflammatory Drugs From the Nasal Region to the Brain. Molecular Therapy. 2011; 19:1769–1779. [PubMed: 21915101]
18. Alvarez-Erviti L, Seow Y, Yin H, Betts C, Lakhal S, Wood MJ. Delivery of siRNA to the mouse brain by systemic injection of targeted exosomes. Nature biotechnology. 2011; 29:341–345.
19. Ohno S, Takanashi M, Sudo K, Ueda S, Ishikawa A, Matsuyama N, Fujita K, Mizutani T, Ohgi T, Ochiya T, Gotoh N, Kuroda M. Systemically injected exosomes targeted to EGFR deliver antitumor microRNA to breast cancer cells. Molecular therapy : the journal of the American Society of Gene Therapy. 2013; 21:185–191. [PubMed: 23032975]
20. Tian Y, Li S, Song J, Ji T, Zhu M, Anderson GJ, Wei J, Nie G. A doxorubicin delivery platform using engineered natural membrane vesicle exosomes for targeted tumor therapy. Biomaterials. 2014; 35:2383–2390. [PubMed: 24345736]
21. Lammers T, Kiessling F, Hennink WE, Storm G. Drug targeting to tumors: principles, pitfalls and (pre-) clinical progress. Journal of controlled release : official journal of the Controlled Release Society. 2012; 161:175–187. [PubMed: 21945285]

22. Takahashi Y, Nishikawa M, Shinotsuka H, Matsui Y, Ohara S, Imai T, Takakura Y. Visualization and in vivo tracking of the exosomes of murine melanoma B16-BL6 cells in mice after intravenous injection. Journal of biotechnology. 2013; 165:77–84. [PubMed: 23562828]
23. Lai CP, Mardini O, Ericsson M, Prabhakar S, Maguire CA, Chen JW, Tannous BA, Breakefield XO. Dynamic biodistribution of extracellular vesicles in vivo using a multimodal imaging reporter. ACS nano. 2014; 8:483–494. [PubMed: 24383518]
24. Smyth TJ, Redzic JS, Graner MW, Anchordoquy TJ. Examination of the specificity of tumor cell derived exosomes with tumor cells in vitro. Biochimica et biophysica acta. 2014; 1838:2954–2965. [PubMed: 25102470]
25. Fevrier B, Vilette D, Archer F, Loew D, Faigle W, Vidal M, Laude H, Raposo G. Cells release prions in association with exosomes. Proceedings of the National Academy of Sciences of the United States of America. 2004; 101:9683–9688. [PubMed: 15210972]
26. Thery C, Regnault A, Garin J, Wolfers J, Zitvogel L, Ricciardi-Castagnoli P, Raposo G, Amigorena S. Molecular characterization of dendritic cell-derived exosomes. Selective accumulation of the heat shock protein hsc73. The Journal of cell biology. 1999; 147:599–610. [PubMed: 10545503]
27. Bligh EG, Dyer WJ. A rapid method of total lipid extraction and purification. Canadian journal of biochemistry and physiology. 1959; 37:911–917. [PubMed: 13671378]
28. Wubbolts R, Leckie RS, Veenhuizen PT, Schwarzmann G, Mobius W, Hoernschemeyer J, Slot JW, Geuze HJ, Stoorvogel W. Proteomic and biochemical analyses of human B cell-derived exosomes. Potential implications for their function and multivesicular body formation. The Journal of biological chemistry. 2003; 278:10963–10972. [PubMed: 12519789]
29. Laulagnier K, Motta C, Hamdi S, Roy S, Fauvelle F, Pageaux JF, Kobayashi T, Salles JP, Perret B, Bonnerot C, Record M. Mast cell- and dendritic cell-derived exosomes display a specific lipid composition and an unusual membrane organization. The Biochemical journal. 2004; 380:161–171. [PubMed: 14965343]
30. Laulagnier K, Vincent-Schneider H, Hamdi S, Subra C, Lankar D, Record M. Characterization of exosome subpopulations from RBL-2H3 cells using fluorescent lipids. Blood cells, molecules & diseases. 2005; 35:116–121.
31. Subra C, Laulagnier K, Perret B, Record M. Exosome lipidomics unravels lipid sorting at the level of multivesicular bodies. Biochimie. 2007; 89:205–212. [PubMed: 17157973]
32. Trajkovic K, Hsu C, Chiantia S, Rajendran L, Wenzel D, Wieland F, Schwille P, Brugger B, Simons M. Ceramide triggers budding of exosome vesicles into multivesicular endosomes. Science. 2008; 319:1244–1247. [PubMed: 18309083]
33. Thakur ML, Lavender JP, Arnot RN, Silvester DJ, Segal AW. Indium-111-labeled autologous leukocytes in man. Journal of nuclear medicine : official publication, Society of Nuclear Medicine. 1977; 18:1014–1021.
34. Abatan OI, Welch KB, Nemzek JA. Evaluation of saphenous venipuncture and modified tail-clip blood collection in mice. Journal of the American Association for Laboratory Animal Science : JAALAS. 2008; 47:8–15. [PubMed: 18459706]
35. Roscoe, B. Jackson Memorial Laboratory. In: Green, EL., editor. Biology of the laboratory mouse. 2d ed.. New York: Blakiston Division; 1966.
36. Haran G, Cohen R, Bar LK, Barenholz Y. Transmembrane ammonium sulfate gradients in liposomes produce efficient and stable entrapment of amphipathic weak bases. Biochimica et biophysica acta. 1993; 1151:201–215. [PubMed: 8373796]
37. Fritze A, Hens F, Kimpfler A, Schubert R, Peschka-Suss R. Remote loading of doxorubicin into liposomes driven by a transmembrane phosphate gradient. Biochimica et biophysica acta. 2006; 1758:1633–1640. [PubMed: 16887094]
38. Smyth T, Petrova K, Payton NM, Persaud I, Redzic JS, Graner MW, Smith-Jones P, Anchordoquy TJ. Surface functionalization of exosomes using click chemistry. Bioconjug Chem. 2014; 25:1777–1784. [PubMed: 25220352]
39. Parolini I, Federici C, Raggi C, Lugini L, Palleschi S, De Milito A, Coscia C, Iessi E, Logozzi M, Molinari A, Colone M, Tatti M, Sargiacomo M, Fais S. Microenvironmental pH is a key factor for

exosome traffic in tumor cells. The Journal of biological chemistry. 2009; 284:34211–34222. [PubMed: 19801663]

40. Kamoun WS, Chae SS, Lacorre DA, Tyrrell JA, Mitre M, Gillissen MA, Fukumura D, Jain RK, Munn LL. Simultaneous measurement of RBC velocity, flux, hematocrit and shear rate in vascular networks. Nature methods. 2010; 7:655–660. [PubMed: 20581828]
41. Tian T, Wang Y, Wang H, Zhu Z, Xiao Z. Visualizing of the cellular uptake and intracellular trafficking of exosomes by live-cell microscopy. Journal of cellular biochemistry. 2010; 111:488–496. [PubMed: 20533300]
42. Hood JL, Pan H, Lanza GM, Wickline SA. I. Consortium for Translational Research in Advanced. Nanomedicine, Paracrine induction of endothelium by tumor exosomes. Laboratory investigation; a journal of technical methods and pathology. 2009; 89:1317–1328.
43. Fanciullino R, Mollard S, Correard F, Giacometti S, Serdjebi C, Iliadis A, Ciccolini J. Biodistribution, Tumor Uptake and Efficacy of 5-FU-Loaded Liposomes: Why Size Matters. Pharmaceutical research. 2014
44. Tang J, Fu H, Kuang Q, Zhang L, Zhang Q, Liu Y, Ran R, Gao H, Zhang Z, He Q. Liposomes co-modified with cholesterol anchored cleavable PEG and octaarginines for tumor targeted drug delivery. Journal of drug targeting. 2014; 22:313–326. [PubMed: 24404866]
45. Phillips WT. Delivery of gamma-imaging agents by liposomes. Advanced drug delivery reviews. 1999; 37:13–32. [PubMed: 10837724]
46. Chow TH, Lin YY, Hwang JJ, Wang HE, Tseng YL, Wang SJ, Liu RS, Lin WJ, Yang CS, Ting G. Improvement of biodistribution and therapeutic index via increase of polyethylene glycol on drug-carrying liposomes in an HT-29/luc xenografted mouse model. Anticancer research. 2009; 29:2111–2120. [PubMed: 19528471]
47. Datz FL. Indium-111-labeled leukocytes for the detection of infection: current status. Seminars in nuclear medicine. 1994; 24:92–109. [PubMed: 8023176]
48. Gabizon A, Papahadjopoulos D. Liposome formulations with prolonged circulation time in blood and enhanced uptake by tumors. Proceedings of the National Academy of Sciences of the United States of America. 1988; 85:6949–6953. [PubMed: 3413128]
49. Weinstein JN, Magin RL, Cysyk RL, Zaharko DS. Treatment of solid L1210 murine tumors with local hyperthermia and temperature-sensitive liposomes containing methotrexate. Cancer research. 1980; 40:1388–1395. [PubMed: 6892792]
50. Goren D, Horowitz AT, Zalipsky S, Woodle MC, Yarden Y, Gabizon A. Targeting of stealth liposomes to erbB-2 (Her/2) receptor: in vitro and in vivo studies. British journal of cancer. 1996; 74:1749–1756. [PubMed: 8956788]
51. Shultz LD, Schweitzer PA, Christianson SW, Gott B, Schweitzer IB, Tennent B, McKenna S, Mobraaten L, Rajan TV, Greiner DL, et al. Multiple defects in innate and adaptive immunologic function in NOD/LtSz-scid mice. Journal of immunology. 1995; 154:180–191.
52. Bradley AJ, Devine DV. The complement system in liposome clearance: Can complement deposition be inhibited? Advanced drug delivery reviews. 1998; 32:19–29. [PubMed: 10837633]
53. Bradley AJ, Devine DV, Ansell SM, Janzen J, Brooks DE. Inhibition of liposome-induced complement activation by incorporated poly(ethylene glycol)-lipids. Archives of biochemistry and biophysics. 1998; 357:185–194. [PubMed: 9735159]
54. Alving CR, Richards RL, Guirguis AA. Cholesterol-dependent human complement activation resulting in damage to liposomal model membranes. Journal of immunology. 1977; 118:342–347.
55. Roerdink F, Wassef NM, Richardson EC, Alving CR. Effects of negatively charged lipids on phagocytosis of liposomes opsonized by complement. Biochimica et biophysica acta. 1983; 734:33–39. [PubMed: 6615828]
56. Richards RL, Habbersett RC, Scher I, Janoff AS, Schieren HP, Mayer LD, Cullis PR, Alving CR. Influence of vesicle size on complement-dependent immune damage to liposomes. Biochimica et biophysica acta. 1986; 855:223–230. [PubMed: 3753881]
57. Chonn A, Cullis PR, Devine DV. The role of surface charge in the activation of the classical and alternative pathways of complement by liposomes. Journal of immunology. 1991; 146:4234–4241.
58. Aung T, Chapuy B, Vogel D, Wenzel D, Oppermann M, Lahmann M, Weinhage T, Menck K, Hupfeld T, Koch R, Trumper L, Wulf GG. Exosomal evasion of humoral immunotherapy in

aggressive B-cell lymphoma modulated by ATP-binding cassette transporter A3. Proceedings of the National Academy of Sciences of the United States of America. 2011; 108:15336–15341. [PubMed: 21873242]

59. Wang AL, Lukas TJ, Yuan M, Du N, Tso MO, Neufeld AH. Autophagy and exosomes in the aged retinal pigment epithelium: possible relevance to drusen formation and age-related macular degeneration. PloS one. 2009; 4:e4160. [PubMed: 19129916]
60. Allen TM, Cleland LG. Serum-induced leakage of liposome contents. Biochimica et biophysica acta. 1980; 597:418–426. [PubMed: 7370258]
61. Frezard F, Santaella C, Montisci MJ, Vierling P, Riess JG. Fluorinated phosphatidylcholine-based liposomes: H+/Na+ permeability, active doxorubicin encapsulation and stability, in human serum. Biochimica et biophysica acta. 1994; 1194:61–68. [PubMed: 8075142]
62. Hegmans JP, Bard MP, Hemmes A, Luider TM, Kleijmeer MJ, Prins JB, Zitvogel L, Burgers SA, Hoogsteden HC, Lambrecht BN. Proteomic analysis of exosomes secreted by human mesothelioma cells. The American journal of pathology. 2004; 164:1807–1815. [PubMed: 15111327]
63. Raimondo F, Morosi L, Chinello C, Magni F, Pitto M. Advances in membranous vesicle and exosome proteomics improving biological understanding and biomarker discovery. Proteomics. 2011; 11:709–720. [PubMed: 21241021]
64. Thery C, Ostrowski M, Segura E. Membrane vesicles as conveyors of immune responses. Nature reviews. Immunology. 2009; 9:581–593.
65. Bobrie A, Colombo M, Raposo G, Thery C. Exosome secretion: molecular mechanisms and roles in immune responses. Traffic. 2011; 12:1659–1668. [PubMed: 21645191]
66. Robbins PD, Morelli AE. Regulation of immune responses by extracellular vesicles. Nature reviews. Immunology. 2014; 14:195–208.
67. Allen TM, Chonn A. Large unilamellar liposomes with low uptake into the reticuloendothelial system. FEBS letters. 1987; 223:42–46. [PubMed: 3666140]
68. Allen TM, Austin GA, Chonn A, Lin L, Lee KC. Uptake of liposomes by cultured mouse bone marrow macrophages: influence of liposome composition and size. Biochimica et biophysica acta. 1991; 1061:56–64. [PubMed: 1995057]
69. Ishida T, Harashima H, Kiwada H. Liposome clearance. Bioscience reports. 2002; 22:197–224. [PubMed: 12428901]
70. Gabizon A, Papahadjopoulos D. The role of surface charge and hydrophilic groups on liposome clearance in vivo. Biochimica et biophysica acta. 1992; 1103:94–100. [PubMed: 1309663]
71. Miyanishi M, Tada K, Koike M, Uchiyama Y, Kitamura T, Nagata S. Identification of Tim4 as a phosphatidylserine receptor. Nature. 2007; 450:435–439. [PubMed: 17960135]
72. Marder SR, Chenoweth DE, Goldstein IM, Perez HD. Chemotactic responses of human peripheral blood monocytes to the complement-derived peptides C5a and C5a des Arg. Journal of immunology. 1985; 134:3325–3331.
73. Scieszka JF, Maggiora LL, Wright SD, Cho MJ. Role of complements C3 and C5 in the phagocytosis of liposomes by human neutrophils. Pharmaceutical research. 1991; 8:65–69. [PubMed: 1826557]
74. Miller ME, Nilsson UR. A familial deficiency of the phagocytosis-enhancing activity of serum related to a dysfunction of the fifth component of complement (C5). The New England journal of medicine. 1970; 282:354–358. [PubMed: 5411128]
75. Dunkelberger JR, Song WC. Complement and its role in innate and adaptive immune responses. Cell research. 2010; 20:34–50. [PubMed: 20010915]
76. Yu S, Liu C, Su K, Wang J, Liu Y, Zhang L, Li C, Cong Y, Kimberly R, Grizzle WE, Falkson C, Zhang HG. Tumor exosomes inhibit differentiation of bone marrow dendritic cells. Journal of immunology. 2007; 178:6867–6875.
77. Xiang X, Poliakov A, Liu C, Liu Y, Deng ZB, Wang J, Cheng Z, Shah SV, Wang GJ, Zhang L, Grizzle WE, Mobley J, Zhang HG. Induction of myeloid-derived suppressor cells by tumor exosomes, International journal of cancer. Journal international du cancer. 2009; 124:2621–2633. [PubMed: 19235923]

78. Liu Y, Xiang X, Zhuang X, Zhang S, Liu C, Cheng Z, Michalek S, Grizzle W, Zhang HG. Contribution of MyD88 to the tumor exosome-mediated induction of myeloid derived suppressor cells. The American journal of pathology. 2010; 176:2490–2499. [PubMed: 20348242]

79. Morelli AE, Larregina AT, Shufesky WJ, Sullivan ML, Stolz DB, Papworth GD, Zahorchak AF, Logar AJ, Wang Z, Watkins SC, Falo LD Jr, Thomson AW. Endocytosis, intracellular sorting, and processing of exosomes by dendritic cells. Blood. 2004; 104:3257–3266. [PubMed: 15284116]

80. Schenkman S, Araujo PS, Dijkman R, Quina FH, Chaimovich H. Effects of temperature and lipid composition on the serum albumin-induced aggregation and fusion of small unilamellar vesicles. Biochimica et biophysica acta. 1981; 649:633–647. [PubMed: 7317422]

81. Jones MN, Nicholas AR. The effect of blood serum on the size and stability of phospholipid liposomes. Biochimica et biophysica acta. 1991; 1065:145–152. [PubMed: 2059649]

82. Li S, Tseng WC, Stolz DB, Wu SP, Watkins SC, Huang L. Dynamic changes in the characteristics of cationic lipidic vectors after exposure to mouse serum: implications for intravenous lipofection. Gene therapy. 1999; 6:585–594. [PubMed: 10476218]

83. Simberg D, Weisman S, Talmon Y, Faerman A, Shoshani T, Barenholz Y. The role of organ vascularization and lipoplex-serum initial contact in intravenous murine lipofection. The Journal of biological chemistry. 2003; 278:39858–39865. [PubMed: 12869564]

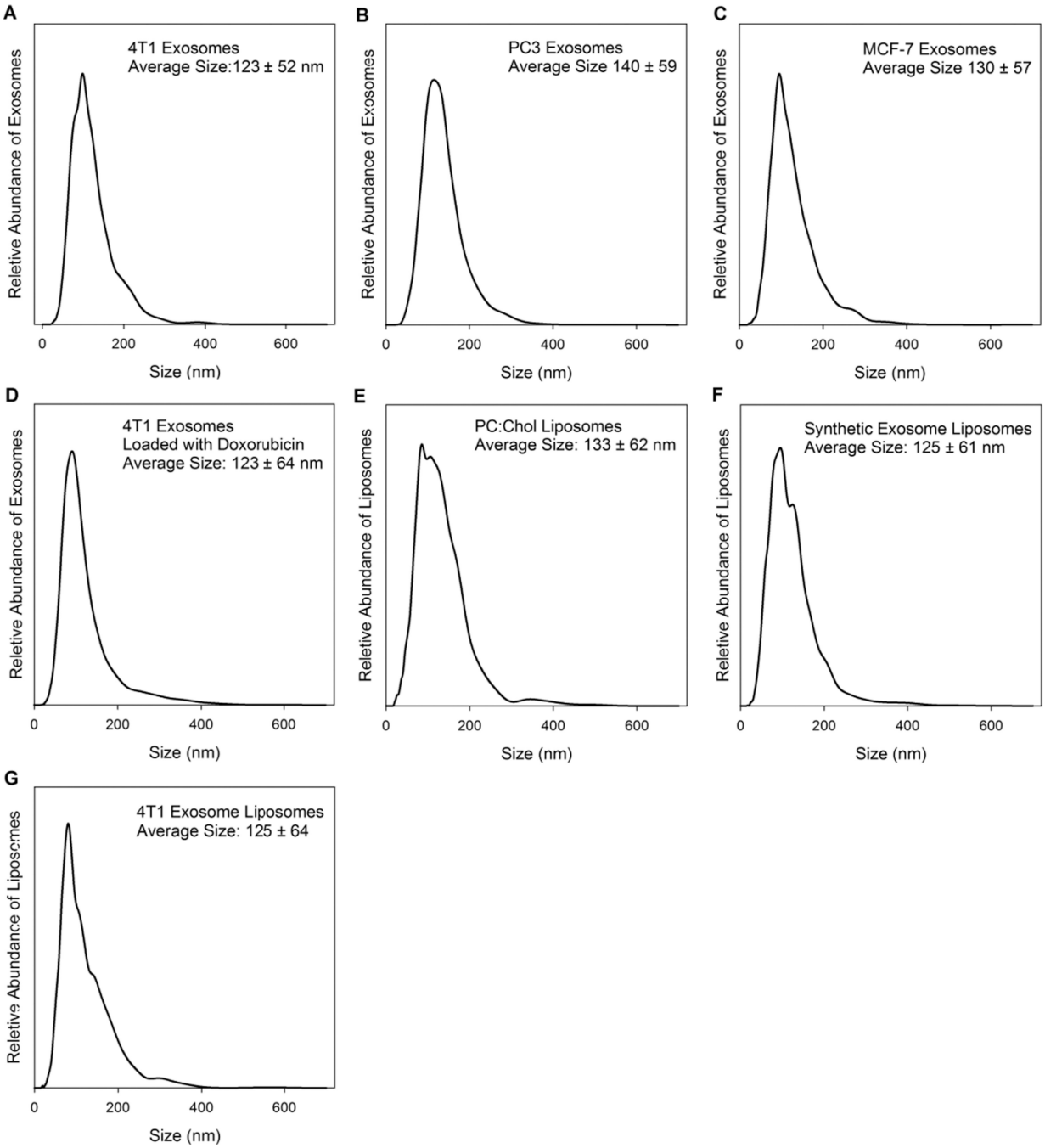

Figure 1.

Size and standard deviations for each exosome or liposome utilized in this work. All measurements were made using a NanoSight NS300.

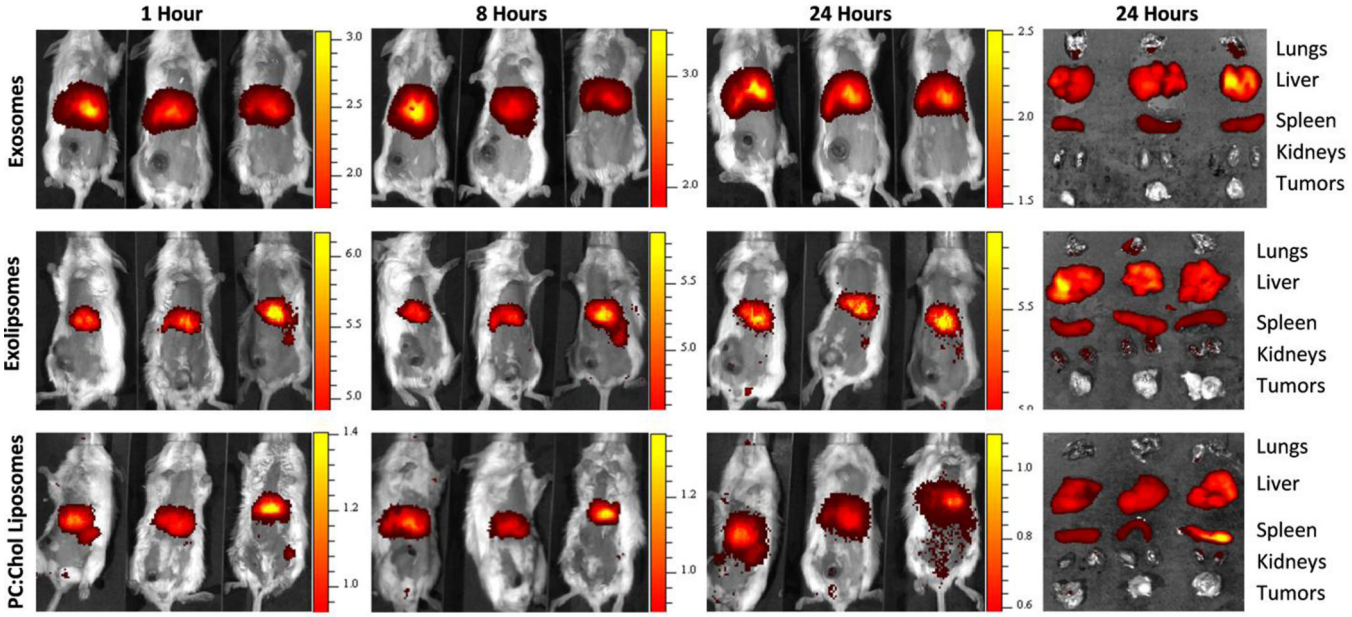

Figure 2.

Balb/c mice bearing 4T1 tumors in their mammary fat pads were injected intravenously with either 60 μg 4T1 exosomes, 60 μg 4T1 exoliposomes, or 60 μg PC:Chol liposomes in a volume of 200 μl PBS. Exosomes and liposomes were labeled with the lipophilic fluorescent probe DIR. A scale of the radiance efficiency is presented to the right of each live mouse image.

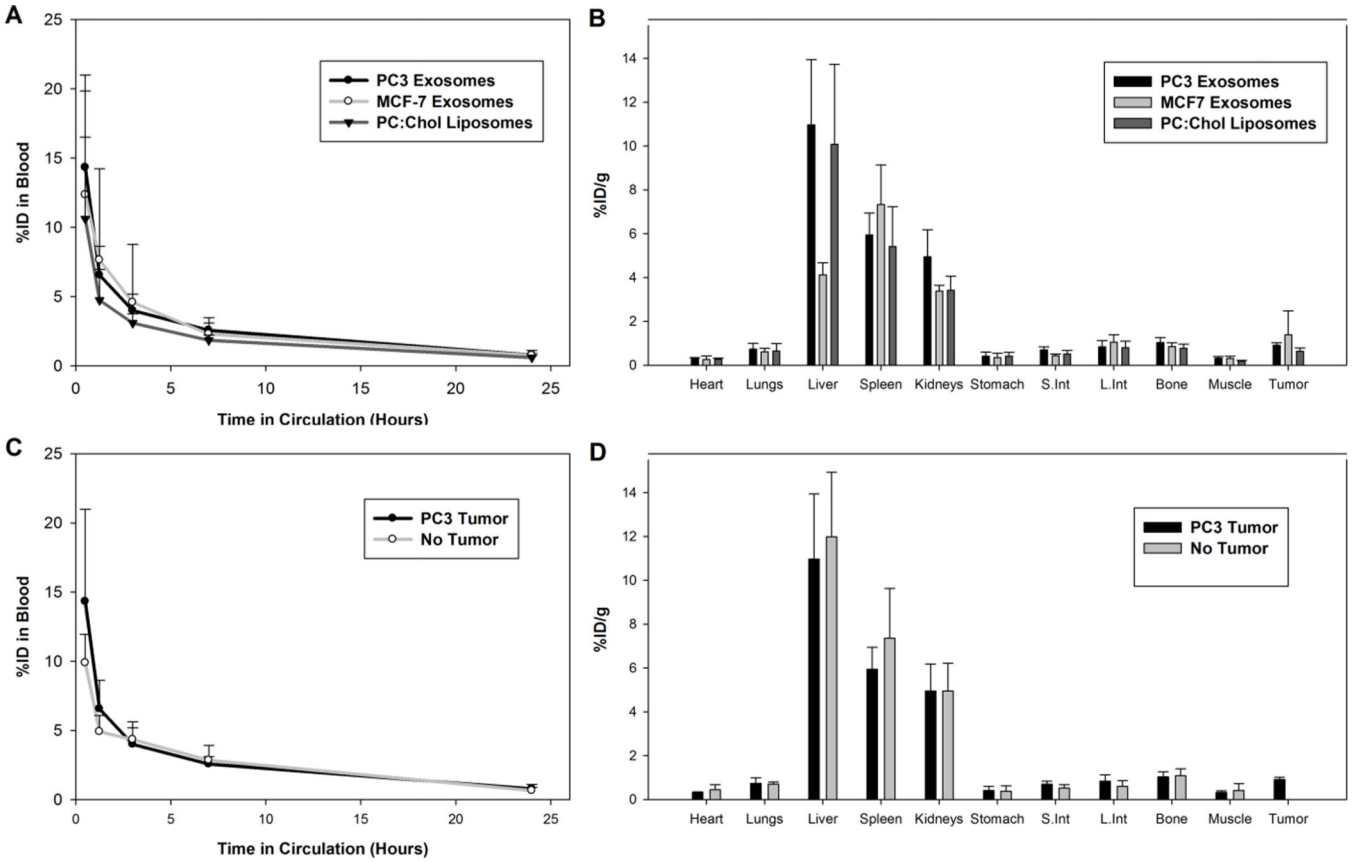

Figure 3.

Exosomes and liposomes radiolabeled with indium-111 were injected into the tail vein of PC3 tumor-bearing mice and non-tumor bearing mice. A) Blood clearance profile of PC3 exosomes, MCF-7 exosomes, and PC:Chol liposomes in PC3 tumor-bearing nude mice. B) Biodistribution of PC3 exosomes, MCF-7 exosomes, and PC:Chol liposomes in PC3 tumor-bearing nude mice 24 hours post injection. C) Blood clearance profile of PC3 exosomes in PC3 tumor-bearing nude mice and non-tumor bearing mice. D) Biodistribution of PC3 exosomes in PC3 tumor-bearing nude mice and non-tumor bearing mice 24 hours post injection.

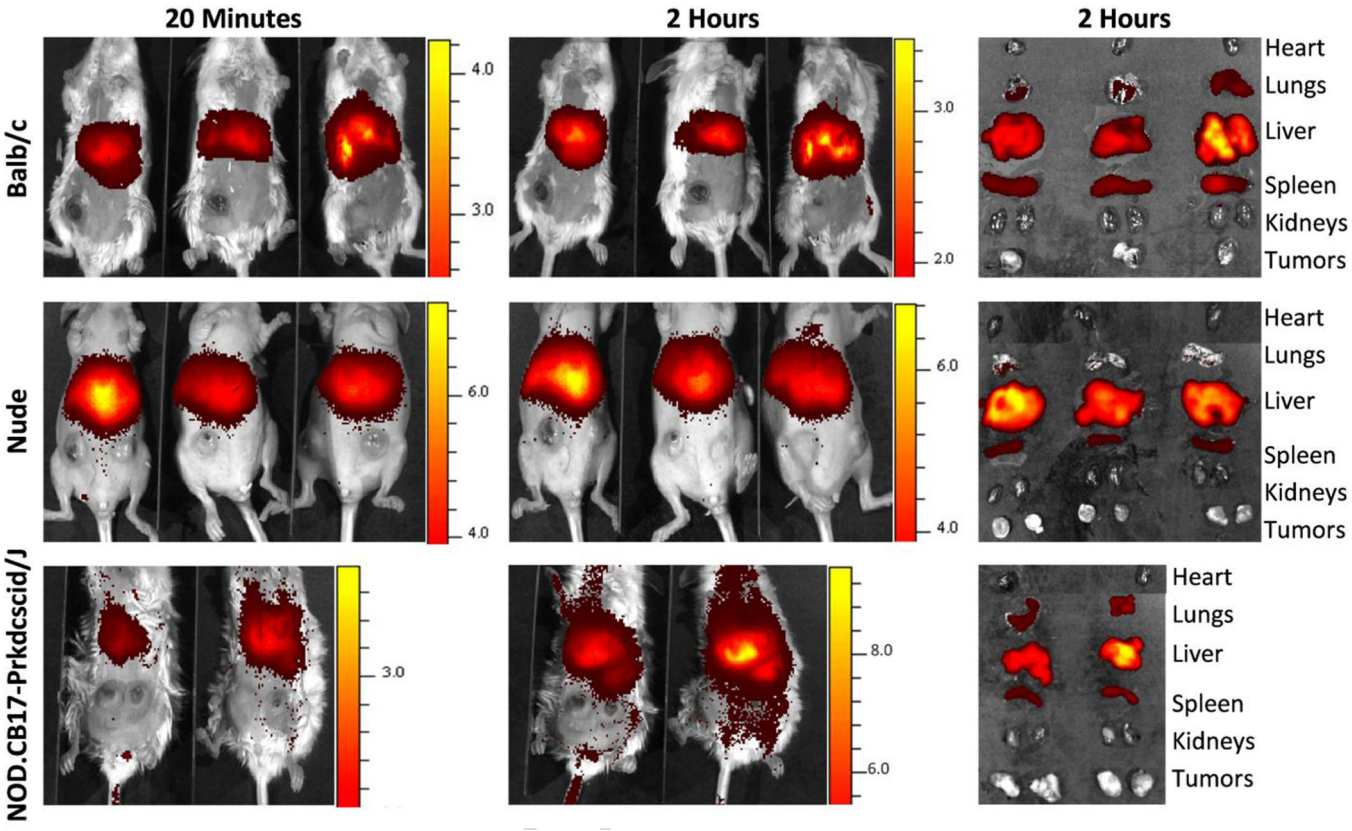

Figure 4.

Intravenous injection of 4T1 exosomes into Balb/c, nude and NOD.CB17-Prkdcscid/J mice. Each mouse strain bearing a 4T1 tumor was intravenously injected with 60 μg 4T1 exosomes labeled with DIR in 100 μl PBS. Mice were imaged at 20 minutes and 2 hours post injection. Organs were excised and imaged after 2 hours. A scale of the radiance efficiency is presented to the right of each live mouse image.

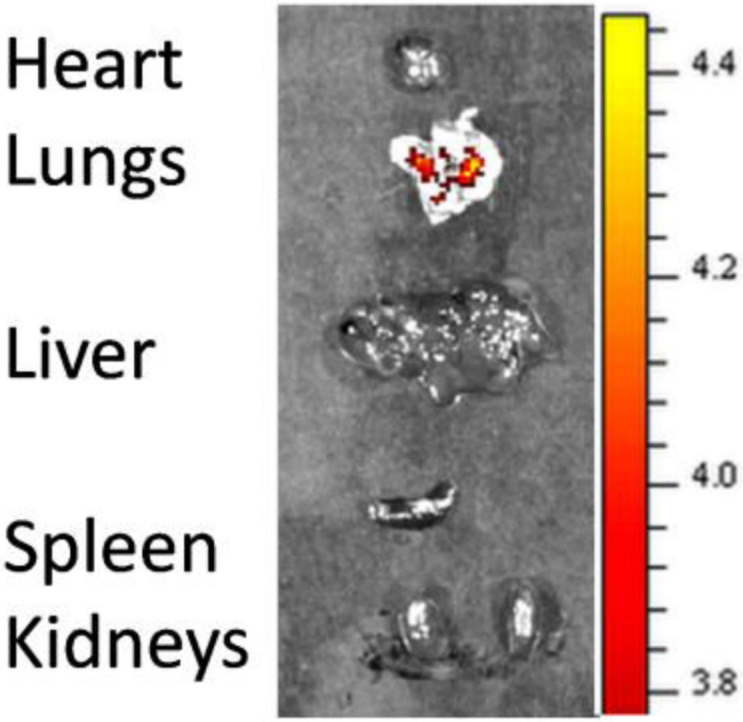

Figure 5.
Excised organs of a Balb/c mouse injected with 400 μg 4T1 exosomes labeled with the fluorescent tracer DIR.

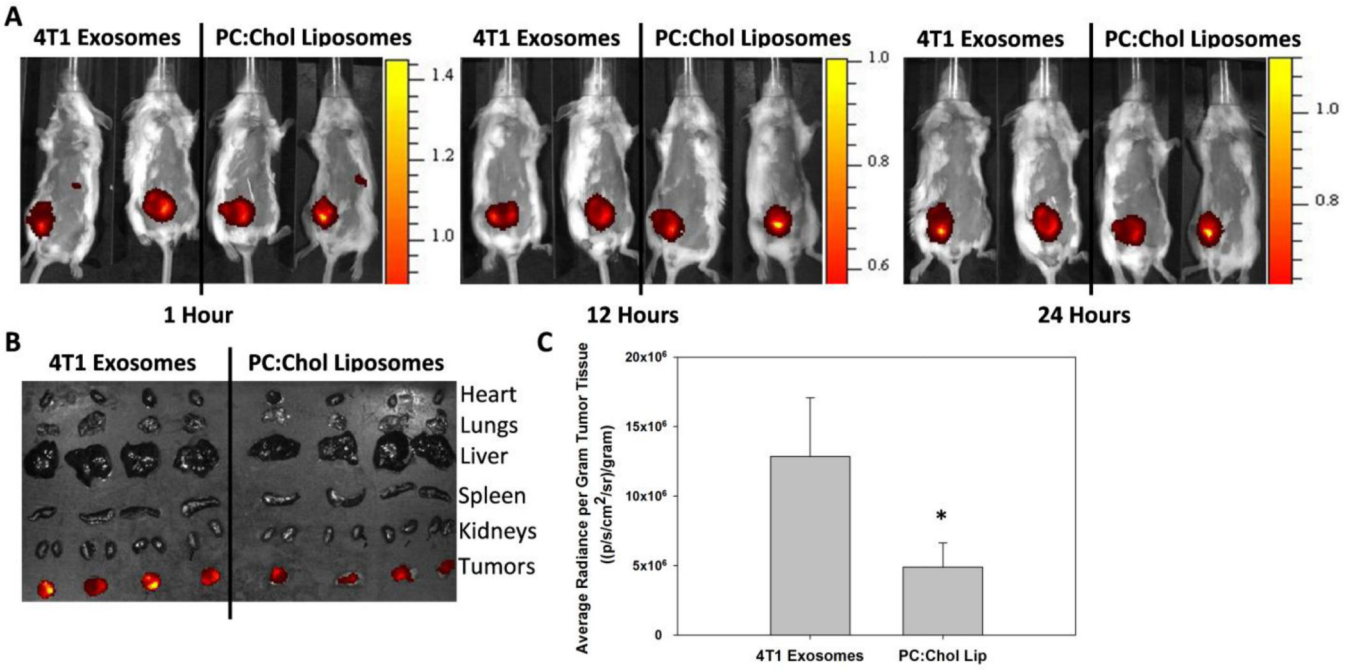

Figure 6.

Intratumoral injection of exosomes and liposomes. A) 60 μg 4T1 exosomes or 60 μg PC:Chol liposomes in 50 μl PBS were injected intratumorally into Balb/c mice bearing a 400 mm^3 4T1 tumor. 4T1 exosomes and PC:Chol liposomes were labeled with equal concentrations of DIR. Two mice from each group were imaged simultaneously for direct comparison. B) The organs from four mice receiving either 4T1 exosomes or PC:Chol liposomes were imaged after 24 h. C) The average radiance per gram of tumor tissue from panel B was quantified using Live Image 4.2 Software. The asterisk indicates a significant difference ($p < 0.05$, student t-test)

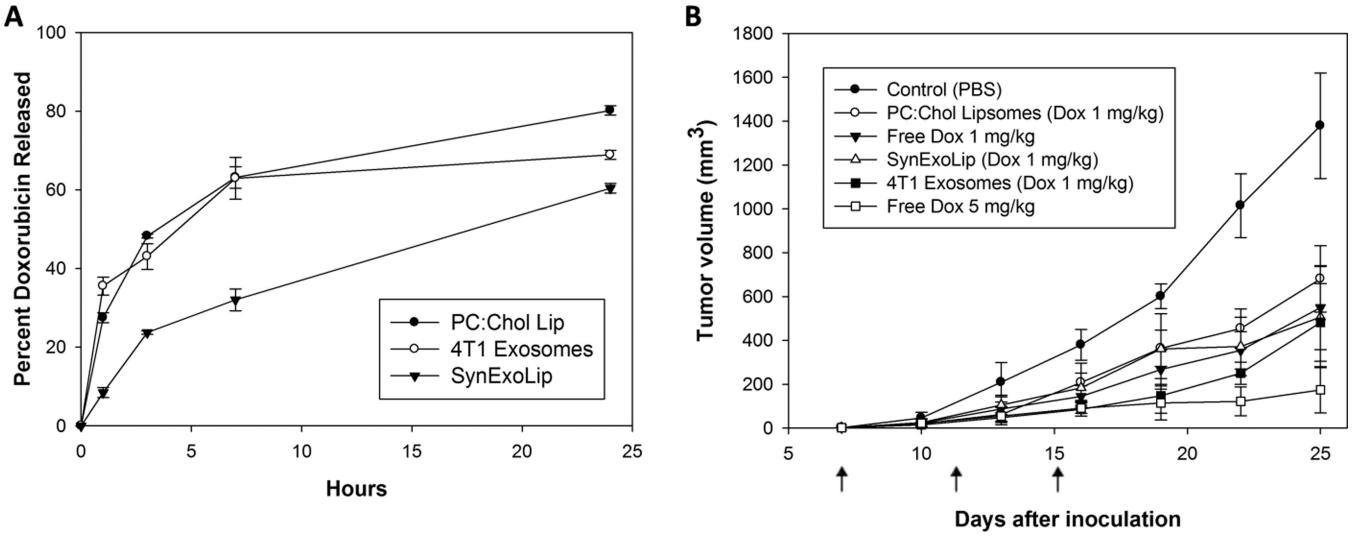

Figure 7.

A) Doxorubicin release profile from 4T1 exosomes, PC:Chol liposomes, and SynExoLiposomes. Exosomes and liposomes were incubated in 50% (v/v) FBS/PBS at 37°C for 24 hours. B) Balb/c mice inoculated with 4T1 tumors were randomly divided into six groups. Each group of six mice received one of the following intratumoral injections: Control (PBS), PC:Chol liposomes loaded with 1 mg/kg doxorubicin, free doxorubicin 1 mg/kg, SynExoLiposomes loaded with 1 mg/kg doxorubicin, 4T1 exosomes loaded with 1 mg/kg doxorubicin, and free doxorubicin 5 mg/kg. Treatment was administered on days 7, 11, and 15 (arrows).